

CHARACTERIZATION OF PIGMENT-BINDING MEDIA SYSTEMS - COMPARISON OF NON-INVASIVE IN-SITU REFLECTION FTIR WITH TRANSMISSION FTIR MICROSCOPY

TECHNICAL PAPER

Wilfried Vetter, Manfred Schreiner

This paper is based on a presentation at the 9th international conference of the Infrared and Raman Users' Group (IRUG) in Buenos Aires, Argentina, 3-6 March 2010.

Guest editor:
Prof. Dr. Marta S. Maier

Institute of Science and Technology in Art, Academy of Fine Arts, Vienna, Austria

corresponding author:
w.vetter@akbild.ac.at

A novel external reflection FTIR device, which enables non-destructive analyses in the region from 4000-450 cm⁻¹ with a measuring point diameter of approximately 5 mm, was tested for the identification of pigments and binding media in two modern paintings and several mockups with traditional pigment-binding media combinations. Comparative measurements were carried out with minute samples using a diamond cell for transmission FTIR microscopy. The results were interpreted by comparison to database spectra measured in transmission mode.

The appearance of distorted peaks in raw reflection spectra impedes a direct comparison with the collected spectra in the transmission mode. Best matches with database spectra were obtained applying the Kramers-Kronig transformation to the reflection spectra of substances showing narrow bands, particularly in the region of about 1900 to 580 cm⁻¹. In the case of modern paintings a good match between transmission and reflection data could be achieved in the fingerprint region. It was possible to identify organic pigments PY 3 (Pigment Yellow 3) and PR 4 (Pigment Red 4) as well as calcite and PVAc (polyvinyl acetate). The identification of materials used for preparation of the mockups was successful for lead white, calcite, Prussian blue, indigo, ultramarine, azurite, malachite, Arabic gum and linseed oil, whereas the transformed spectra of cobalt blue, Naples yellow and especially of smalt and the proteinaceous binding media could not be identified using database spectra.

1 Introduction

Fourier Transform Infrared (FTIR) spectroscopy has been used for decades as a powerful tool for the identification of organic as well as inorganic materials in art and archaeology. Commercial FTIR instruments offer a big variety of methods for different analytical questions in order to generate usable spectra.¹ The diamond cell in a FTIR microscope as well

received: 13.07.2010
accepted: 08.04.2011

key words:
Reflection FTIR, Kramers-Kronig transformation, FTIR microscopy, pigments, binding media

as FTIR-ATR spectroscopy have been applied frequently for the analysis of paintings, both requiring only minute amounts of sample material. In many cases sampling is possible, especially from paintings subjected to a restoration treatment; however, a non-destructive method would be preferable. In recent years, reflection FTIR instruments for non-destructive in-situ analysis of art objects have been developed and applied, controlling the optical path either by mirrors^{2,3} or fibre optics.⁴⁻¹³

Other non-destructive techniques such as X-ray fluorescence analysis (XRF) or UV/Vis spectroscopy have been used for the identification of pigments as well, but both have their limitations. On one hand, XRF (in air) only reveals elements with higher atomic numbers than silicon. On the other hand, UV/Vis spectroscopy may be useful for the identification of both, inorganic and organic pigments or dyes, but not for binding media which show no characteristic absorptions in the respective spectral region. Raman spectroscopy offers the possibility to identify both pigments and binders. Mobile instrumentation is available in the form of hand-held as well as fibre optic instruments which has extended the utility of Raman spectroscopy considerably. The analysis of art objects may be limited by fluorescence phenomena frequently originating from binding media and the risk of damage due to high laser powers.¹⁴

For these reasons, FTIR in the reflection mode seems to be the ideal complementary technique to the aforementioned, providing analytical information about pigments and binding media. However, previous studies^{4,8,10,13,15} demonstrate some drawbacks of this method mainly concerning the distortion of the spectra in the fingerprint region. These distortions are caused by anomalous dispersion due to variations in the refractive index across an absorption band. Therefore, mathematical transformation (Kramers-Kronig transformation) has to be applied in order to gain absorbance-like spectra which may be compared to actual database spectra.¹⁶ However, the transformation will yield accurate results only when diffuse reflectance does not contribute to the analytic signal. This fact raises the questions how far this precondition can be met when paint layers were analyzed and in which way contributing diffuse reflection influences the usability of the results.

In our experiments, we used a novel external reflection FTIR device² to analyze several pigment / binding media combinations and two modern paintings. In all cases also sampling was possible and comparative measurements using a diamond cell for FTIR microscopy could be carried out. Due to the fact that this reflection device controls the beam by mirrors, it offers the possibility to collect mid-infrared spectra in the region from 4000-450 cm⁻¹, which cannot be

achieved with current chalcogenide optical fibres absorbing radiation below 900 cm⁻¹.^{8,16}

2 Experimental

A set of pigment-binding media combinations was prepared on microscope (glass) slides and analyzed by reflection FTIR spectroscopy (r-FTIR) as well as in the FTIR microscope using a diamond cell (μ -FTIR). Table 1 shows the analyzed pigment-binding media combinations. Most of the pigments were mixed with the binder Arabic gum, as the analysis of watercolour paintings is a main focus of our research group. Nevertheless, a combination of lead white with linseed oil as well as with rabbit glue could be included in the studies.

For sample preparation, Arabic gum was mixed with the pigments and distilled water and spread onto the microscope slides utilizing a brush. Oil and glue samples were prepared grinding the binding medium with the pigment on a glass plate and were spread onto the microscope slides utilizing a brush as well.

Furthermore, two graphic art objects on paper, which are attributed to the Austrian contemporary artist Franz West and which were kindly provided by the Franz-West-Archive in Vienna, could be investigated in the studies. Also in that case FTIR spectra were obtained in the reflection mode as well as in the FTIR microscope on minute samples.

| Pigment | Binding medium | Results discussed in |
|---------------|------------------|----------------------|
| lead white | linseed oil | 4.1.1 |
| lead white | rabbit skin glue | 4.1.1 |
| lead white | Arabic gum | 4.1.1 |
| no pigment | Arabic gum | 4.1.2 |
| Prussian blue | Arabic gum | 4.1.3 |
| malachite | Arabic gum | 4.1.3 |
| indigo | Arabic gum | 4.1.4 |
| calcite | Arabic gum | 4.1.5 |
| ultramarine | Arabic gum | 4.1.5 |
| smalt | Arabic gum | 4.1.6 |
| Naples yellow | Arabic gum | 4.1.7 |
| cobalt blue | Arabic gum | 4.1.8 |
| azurite | Arabic gum | 4.1.9 |

Table 1: Overview of the pigment-binding media combinations prepared for the mockups used for r-FTIR and μ -FTIR and discussed in the chapters mentioned.

2.1 Reflection FTIR spectroscopy

Reflection FTIR was carried out with the portable Bruker ALPHA FTIR spectrometer equipped with the novel external reflection module² which kindly was provided for testing by Bruker Optics, Ettlingen, Germany. The reflection module (Figure 1) focuses the beam via mirrors to the sample/object resulting in a beam diameter of about 5 mm. The reflected part is collected also by mirrors and directed to a DTGS-detector. Total reflection spectra (specular and dif-

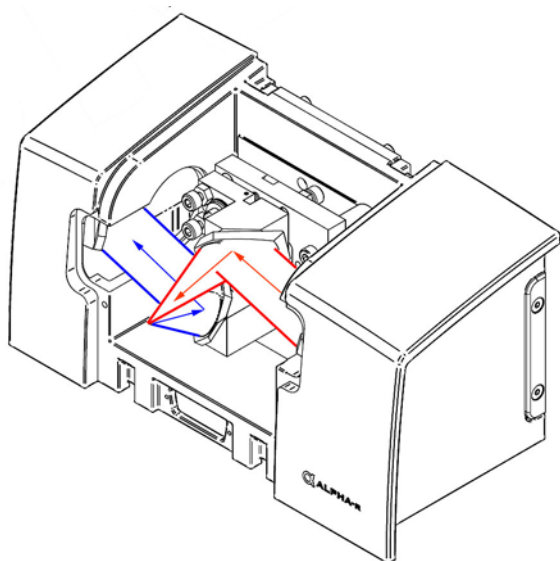


Figure 1: Optical path of the external reflection module. Angle of incidence = angle of reflection = 45°.

use reflection) were collected in-situ in the range of 4000-450 cm^{-1} at a resolution of 4 cm^{-1} over 32 scans. The background was acquired using a gold mirror as reference sample. The total reflection spectra were transformed to absorption index spectra applying the Kramers-Kronig algorithm, which is included in the software package OPUS, version 6.5, used for controlling the ALPHA instrument and data acquisition and evaluation. After the transformation a baseline correction was applied to the absorption index spectra.

2.2 FTIR microscopy with the diamond cell

A Spectrum 2000 FTIR spectrometer (Perkin Elmer, Shelton, CT, USA) in combination with an i-series microscope and a MCT-detector was employed for the FTIR microscopy studies. The spectral range was 4000-580 cm^{-1} with a resolution of 4 cm^{-1} ; 32 scans were acquired for each spectrum. Minute samples were collected at brittle areas of the paint-layer using a syringe needle (0.3 mm diameter) and measured on a diamond cell (SPECTRA TECH, Shelton, CT, USA). The obtained transmission spectra were converted to absorption spectra and will be termed as μ -FTIR spectra in the following parts of the publication. This instrument also was used to measure the reference materials of our institute.¹⁷

2.3 Data evaluation

For the evaluation and interpretation of the absorption index spectra obtained for the mockups as well as the two paintings the following databases were available:

- IRUG – Version 2000¹⁸
- Database of the Institute of Science and Technology in Art (ISTA), Academy of Fine Arts, Vienna, Austria¹⁷
- Tate Organic Pigment Archive¹⁹ for the identification of organic pigments in the two paintings.

3 Results and Discussion

Several spectral features strongly differing from transmission FTIR spectroscopy have been reported for the reflection mode, impeding the interpretation of reflection spectra.¹ Specular reflection leads to first-derivative-like spectral features and strong inverted bands (so called reststrahlen bands), which appear at very strong absorption maxima, particularly of oxyanions.¹⁶ These phenomena are based on the Fresnel equation and thus, Kramers-Kronig transformation can be applied to calculate absorption index spectra, which are comparable to absorption spectra measured in the transmission mode. In order to obtain useful specular reflectance spectra, following conditions must be considered:

1. The optical geometry of the spectrometer has to minimize the fraction of diffusely reflected light (angle of incidence = angle of reflection);
2. The sample surface has to be optically flat (inhibition of diffuse reflection);
3. The sample has to be optically thick in order to avoid interaction of incident radiation with layers or supports below the surface.

Diffuse reflection results from a combined process including reflection, refraction and diffraction of the incident radiation due to interactions with particles of the sample. Diffuse reflection spectra are usually subjected to Kubelka-Munk transformation where the parameter $f[R(\bar{\nu})]$ is derived, which is the ratio of the absorption coefficient $k(\bar{\nu})$ and the scattering coefficient $s(\bar{\nu})$ of the sample ($R(\bar{\nu})$, reflectance at the respective wavenumber). $f[R(\bar{\nu})]$ varies linearly with the concentration enabling quantitative analyses. Diffuse reflection spectra appear to be similar to transmission spectra derived from poorly prepared KBr disks.¹⁶

If the sample of interest is located as a film on a smooth metal surface, the resulting reflection spectra are quite similar to corresponding transmission spectra. In this case, the incident beam is reflected by the metal layer and thus passes through the film twice. This process has been termed as transfection and a good correlation with transmittance spectra without mathematical treatment has been reported analyzing e.g. gold metallic decorations on paintings.⁸

In our experiments, the spectra usually showed typical features of specular reflection and subjecting them to Kramers-Kronig transformation yielded

absorption index spectra similar to transmission derived spectra in many cases. The literature showed that Kramers-Kronig transformation yielded good results processing reflection spectra obtained in a FTIR microscope ($0^\circ/0^\circ$ optical geometry).^{15,20,21-23} Evaluation of reflection spectra calculating “pseudo absorbance” $A' = \log(1/R)$ was preferably used in research studies applying fibre optic instruments^{7-9,11-14,16} combined with PCA (principal component analysis).^{4,8}

3.1 Pigment-binding media mockups

One of the main focuses of our research group is the study of watercolour paintings of the 19th century, hence all pigments have been analyzed in combination with Arabic gum, which is the most important binding medium used in this technique. Additionally, lead white with linseed oil and rabbit skin glue were measured in order to evaluate the effect of different matrices.

3.1.1 Lead white in various binders

The experimental results obtained for the lead white mixtures are summarized in Table 2. It shows the band maxima of the measured reflection-FTIR spectra, the calculated absorption index spectra and the μ -FTIR spectra measured in transmission in comparison to the database spectra of the reference materials. Reststrahlen bands as well as strongly asymmetric bands in the reflection spectrum are not mentioned in the table.

The analyses of the lead white samples demonstrated the importance of interpreting both, the reflection spectrum and the corresponding absorption index spectrum calculated by using the Kramers-Kronig transformation. Vibrations at higher wavenumbers than 1700 cm^{-1} in the reflection spectra of lead white mixed with Arabic gum (3535 , 2919 , 2850 and 1738 cm^{-1}) or rabbit skin glue (2920 , 2850 and 1739 cm^{-1}) were observed at wavenumbers almost similar to those measured in the transmission mode. These band characteristics seem to originate in a contribution of diffusely reflected radiation, which is increased, if the surface roughness is comparable to the infrared wavelength.^{4,10} Below 1700 cm^{-1} absorption index spectra showed more similarities to the spectra measured in the transmission mode, as shown in the Figures 2 and 3.

Arabic gum could not be clearly identified in the mixture due to the overlap with lead white absorptions. Furthermore, the asymmetric stretching vibration of CO_3^{2-} appears distorted in the reflection spectra. However, typical lead white vibrations were found in

the reflection spectrum at 3535 and 1739 cm^{-1} as well as in the absorption index spectrum at 684 and 600 cm^{-1} .

| Lead white in linseed oil – absorption band maxima (cm^{-1}) | | | | |
|-------------------------------------------------------------------------|----------------------------------|-------------|----------------------------------|---------------------------------------|
| r-FTIR reflection spectrum | r-FTIR absorption index spectrum | μ -FTIR | Lead white ISTA17 (Kremer 46000) | Linseed oil IRUG ¹⁸ OF0039 |
| | | 3539 | 3543 | |
| | | | 2964 | |
| | 2931 | 2928 | 2920 | 2927 |
| | 2856 | 2855 | 2851 | 2856 |
| 2430 | 2420 | | 2431 | |
| | 1742 | 1742 | 1738 | 1743 |
| | 1464 | | | 1463 |
| | | 1404 | 1405 | |
| | 1173 | 1167 | | 1168 |
| | 1068 | 1074 | 1074 | |
| | 680 | 683 | 683 | |
| | 597 | 598 | 598 | |

| Lead white in rabbit skin glue – absorption band maxima (cm^{-1}) | | | | |
|------------------------------------------------------------------------------|----------------------------------|-------------|----------------------------------|--------------------------------------------|
| r-FTIR reflection spectrum | r-FTIR absorption index spectrum | μ -FTIR | Lead white ISTA17 (Kremer 46000) | Rabbit skin glue IRUG ¹⁸ PR0017 |
| 3540 | | | 3543 | |
| 3476 | 3170 | 3440 | | 3302 |
| 2959 | 2954 | 2957 | 2964 | |
| 2920 | 2912 | 2923 | 2920 | 2932 |
| 2850 | 2845 | 2855 | 2851 | |
| 2431 | 2400 | 2431 | | |
| 1739 | 1735 | 1733 | 1738 | |
| | 1649 | 1648 | | 1652 |
| | 1557 | 1536 | | 1530 |
| | 1408 | 1407 | 1405 | |
| | 1073 | 1073 | 1074 | |
| | 842 | 841 | 826 | |
| | 683 | 682 | 683 | |
| | 600 | 601 | 598 | |

| Lead white in Arabic gum – absorption band maxima (cm^{-1}) | | | | |
|------------------------------------------------------------------------|----------------------------------|-------------|----------------------------------|--------------------------------------|
| r-FTIR reflection spectrum | r-FTIR absorption index spectrum | μ -FTIR | Lead white ISTA17 (Kremer 46000) | Arabic gum IRUG ¹⁸ CB0012 |
| 3535 | 3525 | 3534 | 3543 | |
| 3470 | 3169 | 3470 | | 3378 |
| 2960 | 2958 | 2959 | 2964 | |
| 2919 | 2913 | 2919 | 2920 | 2928 |
| 2850 | 2846 | 2852 | 2851 | |
| 2428 | 2392 | 2430 | 2431 | |
| 1738 | 1731 | 1738 | 1738 | |
| | | | | 1607 |
| | 1432 | 1407 | 1405 | |
| | 1075 | 1075 | 1074 | 1073 |
| | | 840 | 826 | |
| | 684 | 684 | 683 | |
| | 600 | 600 | 598 | |
| | 600 | 601 | 598 | |

Table 2: Experimental results of r- and μ -FTIR measurements of mockups containing lead white with the binders linseed oil, rabbit skin glue and Arabic gum in comparison to the corresponding spectra in the databases ISTA17 and IRUG.¹⁸

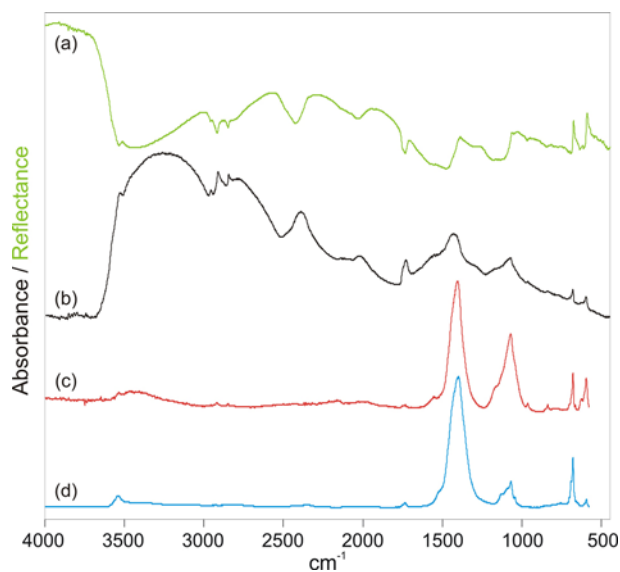


Figure 2: Reflection spectrum of lead white with Arabic gum (a, green), absorption index spectrum calculated from a (b, black) and spectrum obtained by using μ -FTIR in transmission mode (c, red). For comparison the spectrum of the ISTA¹⁷ database obtained for lead white Kremer No. 46000 (d, blue) is also presented.

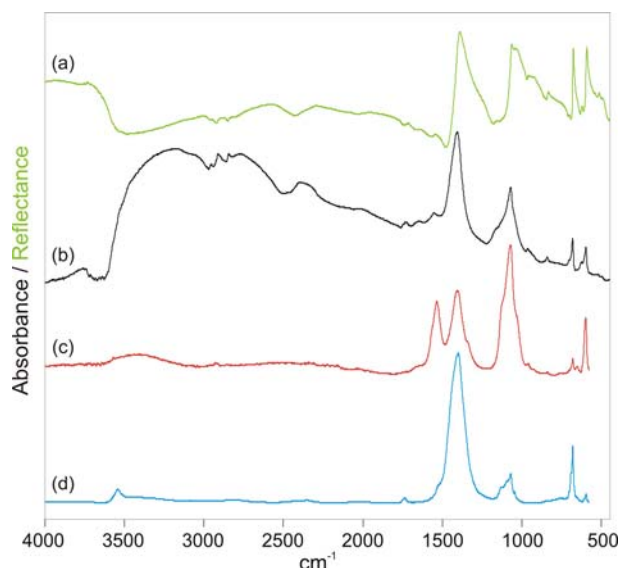


Figure 3: Reflection spectrum of lead white with rabbit skin glue (a, green), absorption index spectrum calculated from a (b, black) and spectrum obtained by using μ -FTIR in transmission mode (c, red). For comparison the spectrum of the ISTA¹⁷ database obtained for lead white Kremer No. 46000 (d, blue) is also presented.

As shown in Figure 3, the μ -FTIR spectrum of lead white with rabbit skin glue revealed a very low content of the binding medium, showing only weak bands for amide I and amide II at 1652 and 1530 cm^{-1} , respectively. Hence, also weak protein bands were observed in the reflection spectrum. The absorption index spectrum appeared almost similar to the μ -FTIR spectrum, although the latter showed a much stronger vibration at about 1540 cm^{-1} . Lead white could be clearly identified by the respective vibrations in the fingerprint region.

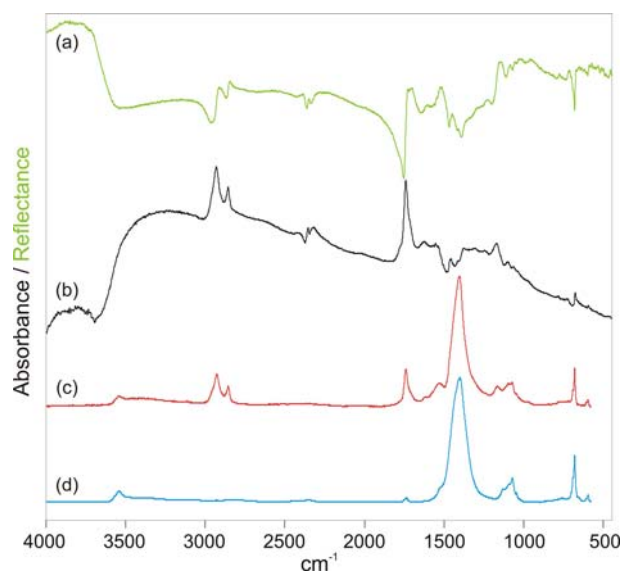


Figure 4: Reflection spectrum of lead white with linseed oil (a, green), absorption index spectrum calculated from a (b, black) and spectrum obtained by using μ -FTIR in transmission mode (c, red). For comparison the spectrum of the ISTA¹⁷ database obtained for lead white Kremer No. 46000 (d, blue) is also presented.

Poor sample preparation impeded the identification of lead white in combination with linseed oil. Sedimentation of lead white could be observed in the approximately 1 mm thick sample and the surface layer mainly consisted of linseed oil. In this case, only two bands of lead white could be registered in the absorption index spectrum at 680 and 598 cm^{-1} (weak), whereas linseed oil could be clearly identified by the C-H stretching bands at 2931 and 2856 cm^{-1} as well as by C=O stretching band at 1742 cm^{-1} (Figure 4). The corresponding transmission sample was taken from below the surface and thus obviously contained more lead white.

3.1.2 Arabic gum

The absorption index spectrum of pure Arabic gum showed similarities with IRUG CB0012 Arabic gum at 1608 cm^{-1} (O-H bending), 1420 cm^{-1} (C-H bending) and around 1074 cm^{-1} (C-O stretching). A remarkable distortion was observed at 1210 cm^{-1} (1193 cm^{-1} in the reflection spectrum, inverted band), which could not be assigned to a particular vibration. A contribution from the glass support can be excluded due to the fact that the main absorption band of glass was observed in the reflection spectrum around 1060 cm^{-1} .

Due to a generally low content in the mixtures, Arabic gum absorptions were hardly detectable since many pigments also show absorptions in similar regions to the characteristic bands of the binder.

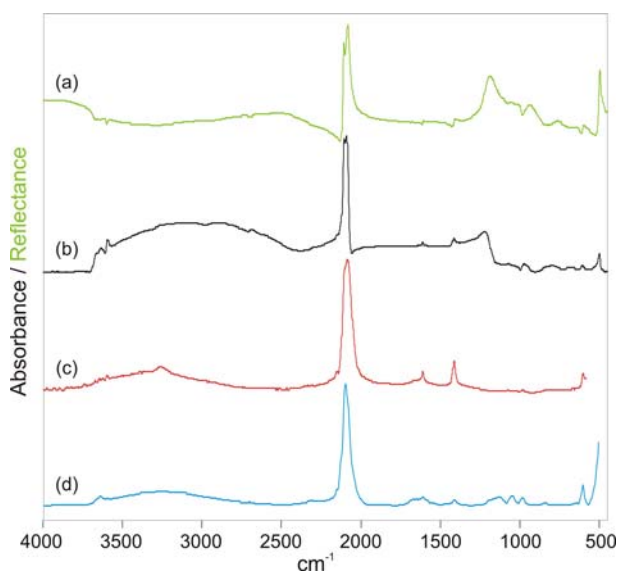


Figure 5: Reflection spectrum of Prussian blue with Arabic gum (a, green), absorption index spectrum calculated from a (b, black) and spectrum obtained by using μ -FTIR in transmission mode (c, red). For comparison the spectrum of the IRUG¹⁸ database MP0047 Prussian blue (d, blue) is also presented.

3.1.3 Prussian blue and malachite

Best matches in the pigment-Arabic gum group were found for Prussian blue (IRUG MP0047) and malachite (IRUG MP0209), which are shown in Figures 5 and 6.

The presence of the strong CN asymmetric stretching vibration at about 2090 cm^{-1} clearly identified Prussian blue and also weaker absorptions were in agreement with the IRUG database and the μ -FTIR spectra (3634 , 1612 , 1416 and 607 cm^{-1}). Similar to the spectrum of pure Arabic gum, a distortion was

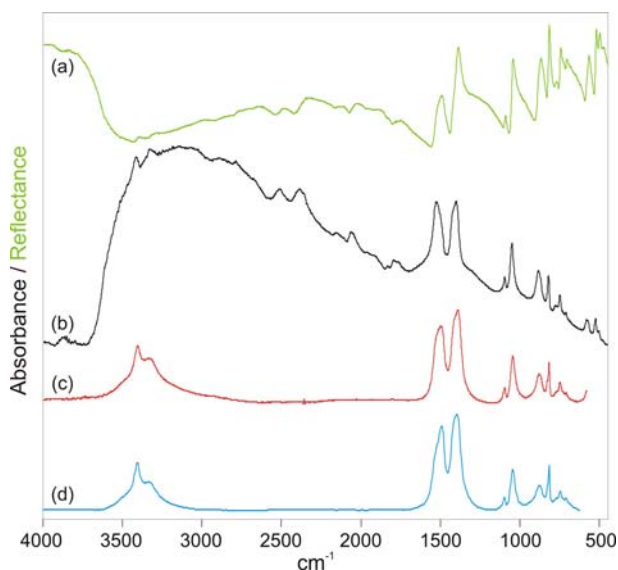


Figure 6: Reflection spectrum of malachite with Arabic gum (a, green), absorption index spectrum calculated from a (b, black) and spectrum obtained by using μ -FTIR in transmission mode (c, red). For comparison the spectrum of the IRUG¹⁸ database MP0209 malachite (d, blue) is also presented.

observed at about 1120 cm^{-1} (1190 cm^{-1} in the reflection spectrum, inverted band).

The reflection spectrum of malachite mainly showed first-derivative-like bands and Kramers-Kronig transformation yielded an absorption index spectrum, where all bands were in agreement with the corresponding IRUG database and the μ -FTIR spectra; only the maximum of the band around 1515 cm^{-1} showed a slight shift to higher wavenumbers (Figure 6).

3.1.4 Indigo

Despite of the very weak intensity of the peaks in the absorption index spectrum, also indigo could be identified without difficulties (Table 3). The poor quality of this spectrum may be attributed to the very thin paint layer and surface roughness of the mockup.

| Indigo in Arabic gum absorption band maxima (cm^{-1}) | | |
|---------------------------------------------------------------------|-------------|-------------------------------------|
| r-FTIR absorption index spectrum | μ -FTIR | Indigo IRUG ¹⁸ OD0192 |
| | 3275 | 3270 |
| | 1626 | 1627 |
| 1616 | 1615 | 1614 |
| 1585 | 1586 | 1585 |
| 1487 | 1484 | 1484 |
| 1465 | 1460 | 1461 |
| 1393 | 1397 | 1395 |
| 1318 | 1318 | 1318 |
| 1300 | 1299 | 1299 |
| 1198 | 1198 | 1198 |
| 1175 | 1174 | 1173 |
| 1127 | 1128 | 1128 |
| 1096 | 1096 | 1096 |
| 1077 | 1075 | 1074 |
| 876 | 879 | 879 |
| 754 | 753 | 753 |
| 712 | 712 | 712 |
| 701 | 699 | 700 |

Table 3: Experimental results of r- and μ -FTIR measurements of indigo with Arabic gum in comparison to the database spectrum IRUG¹⁸ OD0129 Indigo.

3.1.5 Calcite and Ultramarine

Shifts of certain bands in the absorption index spectrum were more pronounced in case of calcite and ultramarine (Figures 7 and 8). Calcite bands at 715 cm^{-1} (in-plane-bending, ν_2) and 880 cm^{-1} (out-of-plane-bending, ν_4) in the absorption index spectrum were in good agreement with the corresponding bands in the IRUG database (MP0232) and the μ -FTIR spectra, whereas the maximum of the asymmetric stretching band of CO_3^{2-} (ν_3) was shifted to 1505 cm^{-1} (at 1412 cm^{-1} in the IRUG database spectrum). This band appeared as strong reststrahlen band in the reflection spectrum, showing two maxima at 1503 and 1408 cm^{-1} , which have been assigned as

the longitudinal and transverse component of the vibration, respectively.¹⁰ As it was the case for lead white, combination bands of the carbonate anion ($\nu_1+\nu_3$ at 2512 cm^{-1} and $\nu_1+\nu_4$ at 1797 cm^{-1}), which only show a weak intensity when measured in transmission mode, are preferably identified in the reflection spectrum appearing at similar wavenumbers with a higher intensity compared to the μ -FTIR and database spectrum. Additionally, the reflection spectra showed two weak bands at 3698 and 3692 cm^{-1} , which are related to O-H stretching of calcium dihydroxide.⁴

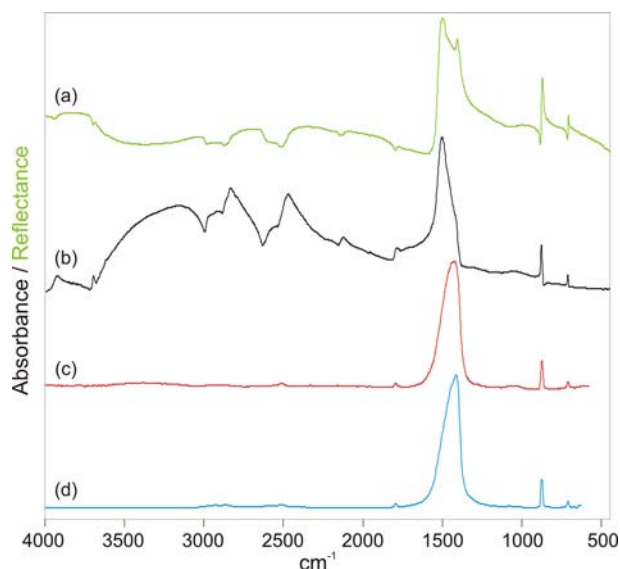


Figure 7: Reflection spectrum of calcite with Arabic gum (a, green), absorption index spectrum calculated from a (b, black) and spectrum obtained by using μ -FTIR in transmission mode (c, red). For comparison the spectrum of the IRUG¹⁸ database MP0232 calcite (d, blue) is also presented.

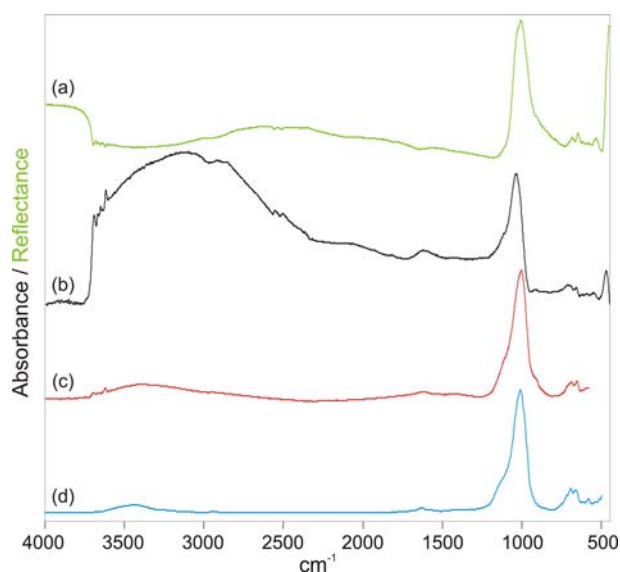


Figure 8: Reflection spectrum of ultramarine with Arabic gum (a, green), absorption index spectrum calculated from a (b, black) and spectrum obtained by using μ -FTIR in transmission mode (c, red). For comparison the spectrum of the IRUG¹⁸ database MP0008 ultramarine (d, blue) is also presented.

The strongest band of ultramarine is the Si-O asymmetric stretching band, showing a maximum at 1012 cm^{-1} in the IRUG database spectrum MP0008 and 1008 cm^{-1} in the μ -FTIR spectrum, appeared as a reststrahlen band (inverted) with the maximum at 1008 cm^{-1} in the reflection spectrum and at 1039 cm^{-1} in the absorption index spectrum (Figure 8). The second strongest band, which is located outside the range of the database spectrum, is the Si-O bending mode with a maximum at 450 cm^{-1} .⁷ Also this vibration was detected inverted in the reflection spectrum at 453 cm^{-1} and as it was the case for the Si-O asymmetric stretching mode, Kramers-Kronig transformation yielded a shifted band at 473 cm^{-1} . In contrast, the bands at 695 and 661 cm^{-1} in the absorption index spectrum were in agreement with the corresponding database spectrum bands (696 and 664 cm^{-1}). The chromophore S_3^- effects a weak absorption at 584 cm^{-1} (ν_3 stretching),⁷ which was barely visible in the reflection spectrum but not the absorption index spectrum. A doublet at 3696 and 3621 cm^{-1} (O-H stretching), as well as two shoulders at 1115 and 916 cm^{-1} indicate the presence of kaolinite, a reagent residue from the manufacturing process of synthetic ultramarine.⁷

3.1.6 Smalt

The maximum of the Si-O antisymmetric stretching band of the smalt database spectra lies between 1030 and 1080 cm^{-1} (IRUG MP0089, MP0094 and MP0100). The reflection spectrum showed this vibration at 1077 cm^{-1} , which is in good accordance to IRUG MP0089. Other vibrations could not be clearly identified in this spectrum, whereas the absorption

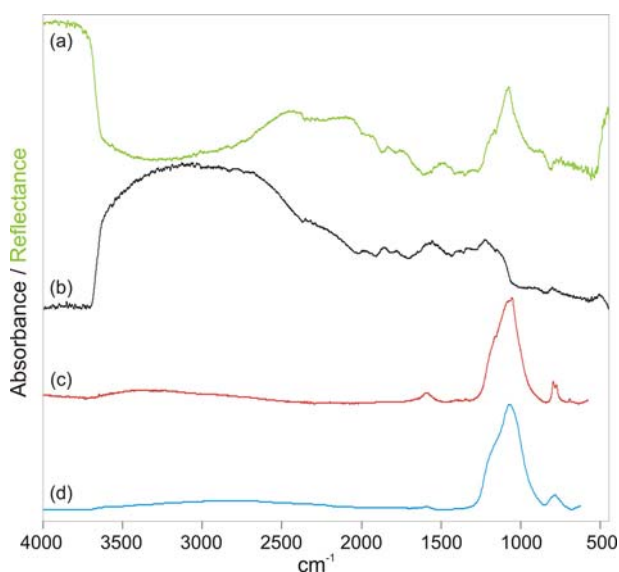


Figure 9: Reflection spectrum of smalt with Arabic gum (a, green), absorption index spectrum calculated from a (b, black) and spectrum obtained by using μ -FTIR in transmission mode (c, red). For comparison the spectrum of the IRUG¹⁸ database MP0089 smalt (d, blue) is also presented.

index spectrum showed the Si-O symmetric stretching band at 805 cm^{-1} . The poor quality of this spectrum results from a very thin layered sample and consequently no vibrations of the cobalt(II) oxide chromophore were visible, which should appear at 664 and 578 cm^{-1} .²⁴ Due to this fact it is likely that the silicate vibrations in this spectrum rather derive from the glass support than from the pigment layer.

3.1.7 Naples yellow

Lead white was identified as component of the Naples yellow sample by μ -FTIR as well as r-FTIR (Figure 10). In general, the absorption bands of Naples yellow (ISTA P00006) interfere with those of lead white at 1405 and 678 cm^{-1} (strongest band of Naples yellow), whereas the latter was much broader than the corresponding lead white band. The absorption index spectrum showed an absorption band at about 680 cm^{-1} with three maxima (698 , 687 and 669 cm^{-1}) and thus is in agreement with the database spectrum. This band was registered as a reststrahlen band at 651 cm^{-1} in the reflection spectrum which was in accordance to the corresponding transmission data. All other bands were related to the lead white content of this sample. Except an absorption at 1333 cm^{-1} , the absorption index spectrum showed spectral features similar to the μ -FTIR spectrum.

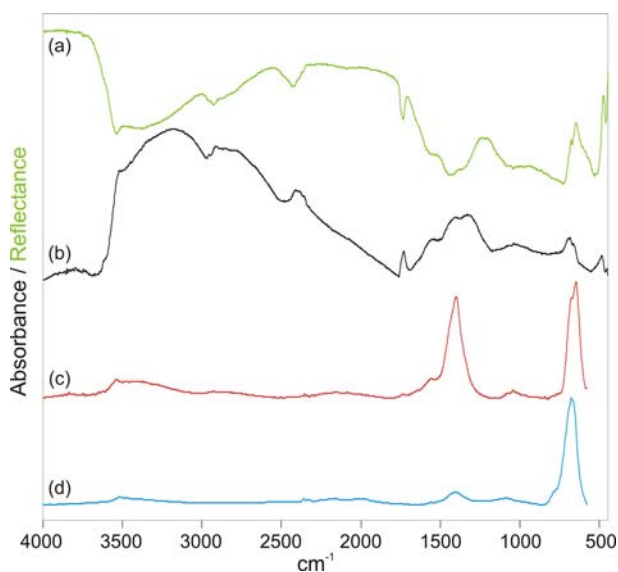


Figure 10: Reflection spectrum of Naples yellow with Arabic gum (a, green), absorption index spectrum calculated from a (b, black) and spectrum obtained by using μ -FTIR in transmission mode (c, red). For comparison the spectrum of the IRUG¹⁸ database MP0006 Naples yellow (d, blue) is also presented.

3.1.8 Cobalt blue

The maximum of the characteristic band of cobalt blue lies around 655 - 670 cm^{-1} (cobalt blue, IRUG MP0095, MP0101 and ISTA P00107). The correspon-

ding band in the absorption index spectrum was detected at about 700 cm^{-1} and in the reflection spectrum at 665 cm^{-1} (inverted, reststrahlen band). In the μ -FTIR spectrum, the maximum of this band was at 551 cm^{-1} . Furthermore, the absorption index spectrum showed two bands at 572 and 519 cm^{-1} , which is outside the range of the database spectra (Figure 11). As it was the case for pure Arabic gum and Prussian blue with Arabic gum, an inverted band could be detected in the reflection spectrum at 1190 cm^{-1} (1213 cm^{-1} in the absorption index spectrum) that could not be attributed (Figure 12).

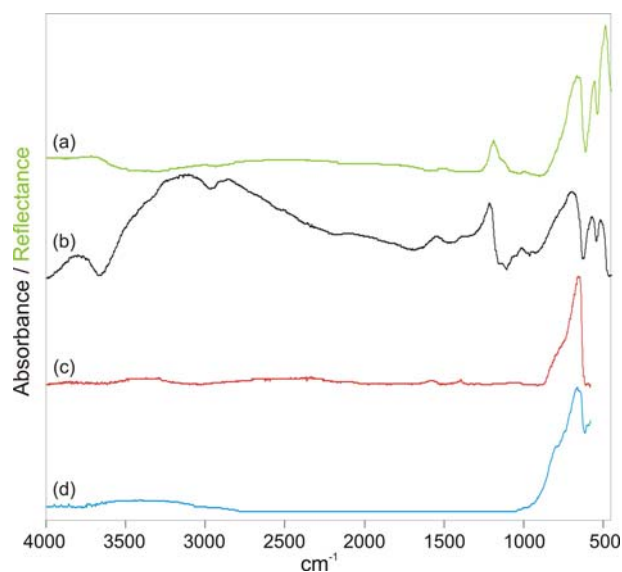


Figure 11: Reflection spectrum of cobalt blue with Arabic gum (a, green), absorption index spectrum calculated from a (b, black) and spectrum obtained by using μ -FTIR in transmission mode (c, red). For comparison the spectrum of the ISTA¹⁷ database P00107 cobalt blue (d, blue) is also presented.

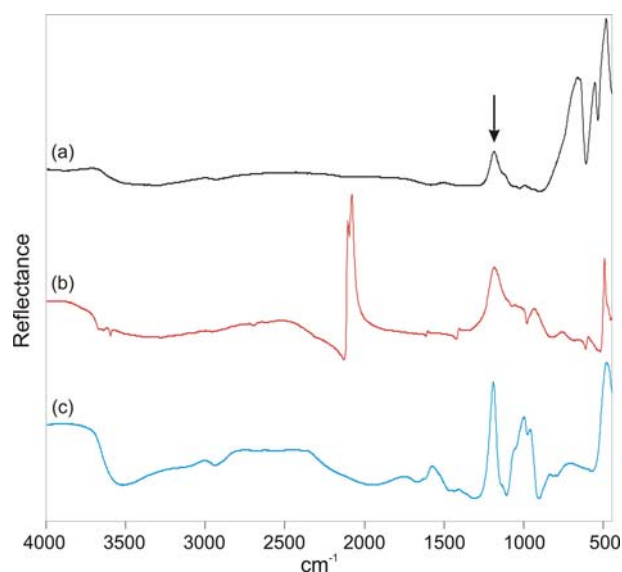


Figure 12: Reflection spectra of cobalt blue with Arabic gum (a, black), Prussian blue with Arabic gum (b, red) and pure Arabic gum (c, blue). The arrow indicates a strong band which appeared in these spectra that could not be assigned to a particular vibration.

3.1.9 Azurite

It has been reported that the carbonate combination band $\nu_1+\nu_3$ at about 2500 cm^{-1} can be used as a marker for azurite rather than the fundamental ν_3 vibration in the region from $1600 - 1400\text{ cm}^{-1}$, which is usually distorted by the reststrahlen effect.^{4,8} Actually the reflection spectrum of azurite with Arabic gum clearly showed the aforementioned bands and the ν_3 vibration was registered inverted, as it is the case for other typical bands of azurite at 956 and 838 cm^{-1} (Figure 13). Contrary, the absorption index spectrum showed no typical bands for azurite and it may be presumed that the diffuse reflection had a high influence during the measurement of this sample.⁴ Furthermore, two bands at 3876 and 3836 cm^{-1} may be related to azurite, since they were also present in reflectance spectra of azurite samples published by other groups.^{4,8} Bands at 3696 , 3620 and 1034 cm^{-1} in the reflection spectrum reveal the presence of kaolinite, which was also confirmed by μ -FTIR data. Great variability in both, position and intensity of azurite bands in the region from 1400 to 1600 cm^{-1} has been reported from a group using a microscope for reflection FTIR analysis of polished cross-sections.¹⁵ These variations have been ascribed to polarization phenomena connected to different orientations of single azurite crystals analyzed. Due to the spot size of the IR beam used in our experiments (approximately 5 mm), we could not observe this effect, assuming an averaged reflection spectrum resulting from a high number of randomly oriented crystals.

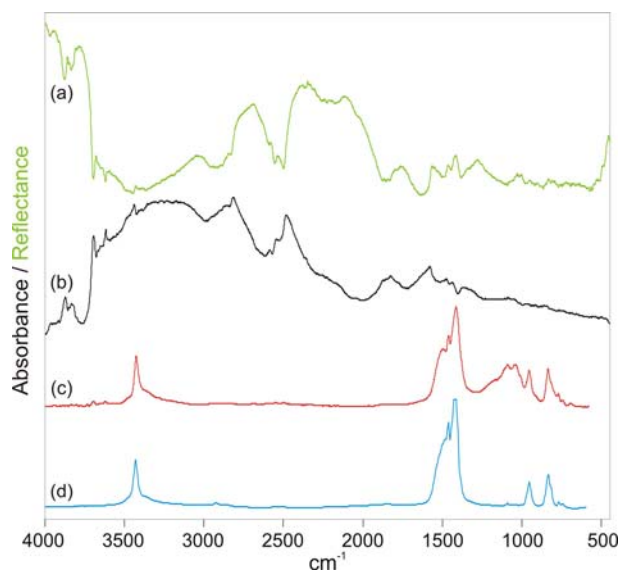


Figure 13: Reflection spectrum of azurite with Arabic gum (a, green), absorption index spectrum calculated from a (b, black) and spectrum obtained by using μ -FTIR in transmission mode (c, red). For comparison the spectrum of the IRUG¹⁸ database MP0001 azurite (d, blue) is also presented.

3.2 Analysis of modern paintings

In addition to the mockups, two paintings on paper could be studied. The paintings which were attributed to the Austrian contemporary artist Franz West (born 1947) were kindly provided by the Franz West archive in Vienna. The artist used colors containing acrylate resin and polyvinyl alcohol as binding medium to paint over pages removed from illustrated magazines. The size was $20 \times 20\text{ cm}$ ("Heute verliebt, morgen betrübt", Inv. No. DN 2181, Figure 14) and $27.5 \times 21\text{ cm}$ (untitled, Inv. No. DN 4956, Figure 15).

Direct comparison of μ -FTIR and r-FTIR demonstrated that similar analytical information can be obtained by the latter method without sampling. Particularly in the fingerprint region below 1800 cm^{-1} , both methods yielded almost similar spectra, when the reflection data was subjected to Kramers-Kronig transformation. It should be mentioned that no varnish was present on the paintings, which possibly may complicate or impede the interpretation of the reflection spectra. The experimental results are summarized in Table 4.

The r-FTIR analysis revealed the presence of calcite at all measuring points, showing typical spectral features at about 2500 and 1795 cm^{-1} in the reflection spectrum as well as at 875 , 715 and in the region from 1390 to 1530 cm^{-1} in the absorption index spectrum. An exception was point 2_red of the object DN 2181, where no calcite could be identified.

Barium sulfate was identified on both paintings, possibly acting as substrate of a lake pigment (Pigment

| | IRUG MP0232 | IRUG MP0293 | IRUG MP0177 | IRUG SR1020 | IRUG SR0008 | Tate Y00003 | Tate R00004 | ISTA OP0918 | IRUG MP0123 |
|------------------|-------------|----------------|-------------|---------------|-------------------|------------------|---------------|------------------|----------------|
| | Calcite | Barium sulfate | Kaolinite | Rhoplex AC-33 | Polyvinyl acetate | Pigment Yellow 3 | Pigment Red 4 | Pigment Red 57:1 | Titanium white |
| Inv. No. DN 2981 | | | | | | | | | |
| 1_white | X / O | | | | X / O | | | | X / O |
| 2_red | | | | X / O | | | | | |
| 3_ruby | X / O | X / O | | | | | | X / O | |
| 4_magenta | X / O | X / O | | | O | | | O | |
| 5_blue | X / O | | | X / O | X | | | | |
| Inv. No. DN 4956 | | | | | | | | | |
| 1_red | X / O | | | | | | X / O | | |
| 2_yellow | X / O | | | | | X / O | | | |
| 3_green | X / O | X / O | | | | X / O | | | |
| 4_blue | X / O | X / O | | | | | | | |
| 5_turquoise | X / O | | X / O | | | | | | |
| 6_white | X / O | | X / O | X / O | | | | | X / O |

Table 4: Materials identified either by r-FTIR-spectroscopy (x) or μ -FTIR spectroscopy (o) by use of the databases ISTA,¹⁷ IRUG¹⁸ and Tate.¹⁹



Figure 14: Painting on paper (Inv. No. DN 2181) with the title "Heute verliebt, morgen betrübt" by the contemporary artist Franz West including the points/areas used for r-FTIR and μ -FTIR.



Figure 15: Painting on paper (Inv. No. DN 4956, untitled) attributed to Franz West including the points/areas used for analysis (r- and μ -FTIR).

Red 57:1 in the object DN 2981 together with calcite) or as extender. It has been reported that Pigment Red 57:1 usually is produced in form of a calcium lake.²⁵ Table 5 shows the bands which can be attributed to barium sulfate from measuring point 3_ruby on object DN 2981 in comparison to the database spectrum of barium sulfate (IRUG MP0293).

| Barium sulfate - absorption band maxima (cm ⁻¹) | | | |
|-------------------------------------------------------------|----------------------------------|-------------|------------------------------|
| r-FTIR reflection spectrum | r-FTIR absorption index spectrum | μ -FTIR | barium sulfate IRUG18 MP0293 |
| 1175 | 1185 | 1180 | 1180 |
| 1117 | 1124 | 1122 | 1111 |
| 1073 | 1094 | 1083 | 1075 |
| 980 | 984 | 984 | 985 |
| 632 | 636 | 635 | 635 |
| 606 | 614 | 610 | 610 |

Table 5: Barium sulfate bands of r- and μ -FTIR measurements of measuring point 3_ruby on object DN 2981 in comparison to the database spectrum IRUG¹⁸ MP0293 barium sulfate.

Kaolinite was identified in DN 4956 point 5_turquoise, the characteristic bands were found at 1038, 1007 and 912 cm⁻¹, appearing as reststrahlen bands in the reflection spectrum, which also showed the O-H stretching vibrations at 3693 and 3626 cm⁻¹. The r- and μ -FTIR spectra of point_5_turquoise show many similarities to the corresponding spectra of point 4_blue and it may be assumed that kaolinite was used for diluting this color in order to achieve the desired hue.

Pigment Yellow 3 (Tate reference database, Y00003) was identified in the object DN 4956 point 2_yellow and point 3_green, whereas a blue component could not be identified on the latter. Figure 16 shows the comparison of the absorption index spectrum of point 2_yellow to the μ -FTIR and the reference database spectra.

The reflection spectrum of point 3_green was in agreement with the bands in the fingerprint region of the database spectrum of Pigment Yellow 3 (plotted in transmission) very precise at 1673, 1339, 1282, 1261, 1232, 1178, 752 and 712 cm⁻¹ (Figure 17),

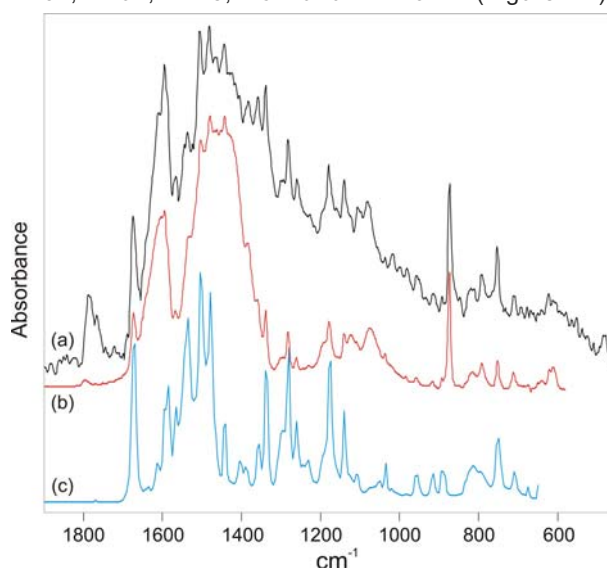


Figure 16: Absorption index spectrum calculated from reflection data of point_2_yellow (a, black) in the object DN 4956 compared to the transmission mode derived μ -FTIR (b, red) and database spectrum (c, blue) of Pigment Yellow 3, Tate reference database¹⁹ Y00003.

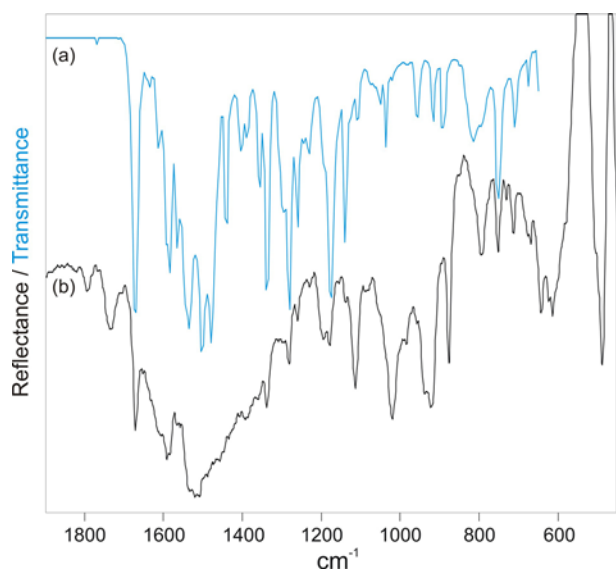


Figure 17: Reflection spectrum of point 3_green (b, black) in the object DN 4956 compared to the reference spectrum (a, blue) of Pigment Yellow 3, Tate database¹⁹ Y00003.

whereas Kramers-Kronig transformation was necessary to correct the first-derivative-like bands of the pigment in the reflection spectrum of point 2_yellow. This result demonstrates a strong influence of the matrix on the appearance of reflection spectra resulting in different contributions of specular and diffuse reflection. In case of point 2_yellow, specular reflection apparently dominates the appearance of the reflection spectrum whereas a transfection¹⁶ phenomenon may be assumed at point 3_green.

Pigment Red 57:1 (also known as Rubine Toner B4), one of the most common organic pigments,²⁵ could be clearly identified on the object DN 2181 at points 3_ruby and 4_magenta by μ -FTIR using the diamond cell, whereas interferences with polyvinyl acetate and calcite from the matrix hampered the interpretation of the reflection spectra. Only weak signals were obtained from the pigment at point 4_magenta. In this case, the higher spatial resolution of the transmission technique enabled the measurement of agglomerated pigment particles and consequently, reduced interferences with the matrix could be observed.

Pigment Red 4, a β -Naphthol pigment,²⁵ clearly was identified together with calcite in the absorption index spectrum of the object DN 4956 point 1_red (Figure 18) which was in agreement with the Tate database spectrum R00004.

The identification of the synthetic binding medium polyvinyl acetate (reference: polyvinyl acetate, IRUG SR0129) was possible for the object DN 2181 at point 1_white (Figure 19), where also calcite was detected. A broad band in the reflection spectrum from about 800 cm^{-1} to lower wavenumbers argues for the presence of rutile as white pigment. In comparison to the

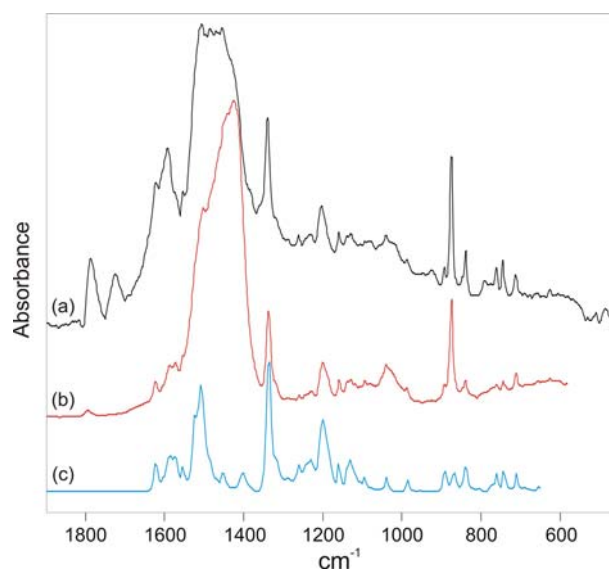


Figure 18: Absorption index spectrum calculated from reflectance data (a, black) and the μ -FTIR-spectrum measured in transmission mode (b, red) of point 1_red on the object DN 4956 compared to the reference spectrum (c, blue) of Pigment Red 4, Tate reference database¹⁹ R00004.

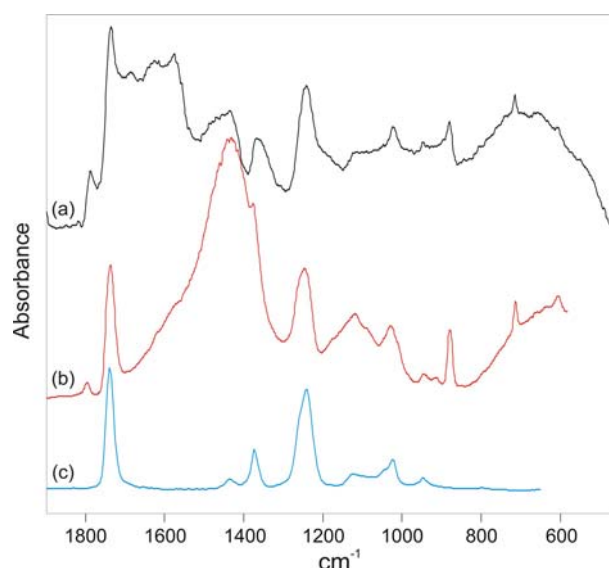


Figure 19: Absorption index spectrum calculated from reflection data (a, black) and the μ -FTIR spectrum measured in transmission (b, red) of point 1_white in the object DN 2181 compared to the reference spectrum (c, blue) of polyvinyl acetate, IRUG¹⁸ SR0129.

μ -FTIR spectrum, additional absorption bands were detected between the carbonyl band of polyvinyl acetate and the carbonate ν_3 band of calcite in the absorption index spectrum, whereas the latter appeared strongly distorted. Polyvinyl acetate was further detected for DN 2181 at point 5_blue but not at point 4_magenta, although it was identified by μ -FTIR there.

A copolymer of ethyl acrylate and methyl methacrylate (Rhoplex AC-33, IRUG SR1020) was utilized by the artist as binding medium for the fluorescent pigment at point 2_red. This synthetic binder also was detect-

ed in the absorption index spectrum of point 5_blue, but not in the corresponding μ -FTIR spectrum.

The reflection spectrum of DN 4956 point 6_white showed a very strong reststrahlen band from about 800 cm^{-1} to lower wavenumbers which could be assigned to rutile. In the absorption index spectrum, only weak signals originated from calcite, kaolinite and Rhoplex AC-33, which clearly were identified in the μ -FTIR spectrum. The strongest absorption bands of calcite and kaolinite (asymmetric stretching of carbonate and silicate) were strongly distorted and consequently, a clear identification was not possible.

4 Conclusions

The study presented illustrates a high potential for the applicability of the tested external reflection device. The method of in-situ reflection FTIR spectroscopy is in general complementary to other non-destructive methods such as XRF or UV/Vis spectroscopy and may contribute important analytical data for the identification of paint materials, especially of such, which cannot be identified with the methods aforementioned (e.g. binding media). The portability and the non-destructive mode of operation of the instrument enables on-site analysis of art objects which cannot be transported for certain reasons and where sampling is not possible. Thus, the field of application is extended to a high degree. In contrast to current fibre optic FTIR instruments, which have a limited spectral range (weak signals below 900 cm^{-1}), the full spectral range from $4000 - 450\text{ cm}^{-1}$ can be evaluated using the tested external reflection instrument.

The frequent appearance of distorted bands indicates a high contribution of specular reflectance in this experimental setting and often necessitates Kramers-Kronig transformation to enable comparison to database spectra derived from transmission measurements. Despite the spectral distortions and inverted bands, a direct evaluation of reflection spectra was successful particularly in the case of pigments containing oxyanions (e.g. carbonates or silicates), as strong inverted bands (reststrahlen bands) showed maxima at similar wavenumbers compared to transmission spectra. Particularly carbonate pigments, which depicted diagnostically useful features in the reflection spectra (combination bands), highlight the necessity to consider both the reflection spectra and the corresponding absorption index spectra for the interpretation of the analytical results.

In addition, we found that a high contribution of the surface layer to the analytical signal may impede the pigment layer analysis of multilayered samples. Another limitation arises from the spot size of the IR

beam in the applied instrument, which was about 5 mm and does not allow the analysis of fine structures on the objects investigated.

Despite all mentioned drawbacks, a good portion of the analyzed materials could be identified and direct comparison to μ -FTIR showed predominance of this method only in a few cases. Also in the case study, where two modern paintings on paper were analyzed, r-FTIR yielded analytical information almost similar to μ -FTIR without sampling.

It can be concluded that the presented technique is convenient as an alternative to micro-destructive transmission FTIR microscopy especially in combination with complementary non-destructive methods.

5 Literature

1. M.R. Derrick, D. Stulik, J.M. Landry, *Infrared Spectroscopy in Conservation Science*, Scientific Tools for Conservation, Getty Conservation Institute, 1999, pp. 43-81.
2. Bruker Optics, Ettlingen, Germany, <http://www.brukeroptics.com/alphaaccessories.html?&L=0&print=1%25252525253F> (accessed 27/10/2009)
3. N. Ferrer, A. Vila, *Fourier transform infrared spectroscopy applied to ink characterization of one-penny postage stamps printed 1841–1880*, Anal. Chim. Acta 2006, **555**, 161-166.
4. F. Rosi, A. Daveri, C. Miliani, G. Verri, P. Benedetti, F. Pique, B.G. Brunetti, A. Sgamellotti, *Non-invasive identification of organic materials in wall paintings by fiber optic reflectance infrared spectroscopy: a statistical multivariate approach*, Anal. Bioanal. Chem. 2009, **395**, 2097-2106.
5. F. Rosi, A. Burnstock, K.J. Van den Berg, C. Miliani, B.G. Brunetti, A. Sgamellotti, *A non-invasive XRF study supported by multivariate statistical analysis and reflectance FTIR to assess the composition of modern painting materials*, Spectrochim. Acta A 2009, **71**, 1655-1662.
6. C. Miliani, F. Rosi, A. Burnstock, B.G. Brunetti, A. Sgamellotti, *Non-invasive in-situ investigations versus micro-sampling: a comparative study on a Renoirs Painting*, Appl. Phys. A 2007, **89**, 849-856.
7. C. Miliani, A. Daveri, B.G. Brunetti, A. Sgamellotti, *CO₂ entrapment in natural ultramarine blue*, Chem. Phys. Lett. 2008, **466**, 148-151.
8. C. Miliani, F. Rosi, I. Borgia, P. Benedetti, B.G. Brunetti, A. Sgamellotti, *Fiber-Optic Fourier Transform Mid-Infrared Reflectance Spectroscopy: A Suitable Technique for in Situ Studies of Mural Paintings*, Appl. Spectrosc. 2007, **61**, 293-299.
9. C. Miliani, B. Doherty, A. Daveri, A. Loesch, H. Ulbricht, B.G. Brunetti, A. Sgamellotti, *In situ non-invasive investigation on the painting techniques of early Meissen Stoneware*, Spectrochim. Acta A 2009, **73**, 587-592.
10. C. Ricci, C. Miliani, B.G. Brunetti, A. Sgamellotti, *Non-invasive identification of surface materials on marble artifacts with fiber optic mid-FTIR reflectance spectroscopy*, Talanta 2006, **69**, 1221-1226.
11. K. Kahrim, A. Daveri, P. Rocchi, G. de Cesare, L. Cartechini, C. Miliani, B.G. Brunetti, A. Sgamellotti, *The application of in situ mid-FTIR fibre-optic reflectance spectroscopy and GC-MS analysis to monitor and evaluate painting cleaning*, Spectrochim. Acta A 2009, **74**, 1182-1188.
12. M. Bacci, M. Fabbri, M. Picollo, S. Porcinai, *Non-invasive fibre optic Fourier transform-infrared reflectance spectroscopy on painted layers. Identification of materials by means of principal component*

- analysis and Mahalanobis distance, *Anal. Chim. Acta* 2001 **446**, 15–21.
13. B. Ormsby, E. Kampasakali, C. Miliani, T. Learner, *An FTIR-Based Exploration of the Effects of WET Cleaning Treatment on Artists' Acrylic emulsion Paint Films*, *e-Preserv. Sci.* 2009, **6**, 186-195.
14. E. Smith, G. Dent, *Modern Raman Spectroscopy: A Practical Approach*, John Wiley & Sons, West Sussex, England, 2006, pp. 28-32.
15. S. Bruni, F. Cariati, F. Casadio, L. Toniolo, *Spectrochemical characterization by micro-FTIR spectroscopy of blue pigments in different polychrome works of art*, *Vibr. Spectrosc.* 1999, **20**, 15-25.
16. P. R. Griffiths, J. A. de Haseth, *Fourier Transform Infrared Spectrometry*, 2nd edition, John Wiley & Sons, Hoboken, New Jersey, 2007, pp. 277-281.
17. Institute of Science and Technology in Art (ISTA), Academy of Fine Arts, Vienna, Austria.
18. IRUG – Version 2000, <http://www.irug.org> (accessed 03/05/2011).
19. Reference database: Tate Organic Pigment Archive, Millbank, London SW1P 4 RG.
20. J. Zieba-Palus, *Examination of spray paints by the use of reflection technique of microinfrared spectroscopy*, *J. Mol. Struct.* 2005, **744–747**, 229–234.
21. A. van Loon, J.J. Boon, *Non-destructive and non-invasive analyses shed light on the realization technique of ancient polychrome prints*, *Spectrochim. Acta A* 2009, **73**, 539-545.
22. J.M. Chalmers, N.J. Everall, S. Ellison, *Specular Reflectance: A Convenient Tool for Polymer Characterisation by FTIR-Microscopy*, *Micron*, 1996, **27**, 315-328.
23. Z.E. Papiaka, K.S. Andrikopoulos, EA. Varella, *Study of the stability of a series of synthetic colorants applied with styrene-acrylic copolymer, widely used in contemporary paintings, concerning the effects of accelerated ageing*, *J. Cult. Her.* 2010, in press, doi:10.1016/j.culher.2010.02.003.
24. D. Jonynaite, J. Senvaitiene, A. Beganskiene, A. Kareiva, *Spectroscopic analysis of blue cobalt smalt pigment*, *Vibr. Spectrosc.* 2010, **52**, 158-162.
25. W. Herbst, K. Hunger, *Industrielle Organische Pigmente*, Zweite Auflage, VCH, Weinheim, 1995.